JOURNAL OF MATERIALS SCIENCE **40** (2005) 2425–2429

Migration of liquid phase in low temperature sintering of AlN

R. FU
College of Material Science and Technology, Nanjing University of Aeronautics and Astronautics, People's Republic of China; Department of Ceramics and Glass Engineering, University of Aveiro, 3810-193 Aveiro, Portugal

K. CHEN
State Key Laboratory of New Ceramics and Fine Processing, Tsinghua University, Beijing 100084, People's Republic of China

S. AGATHOPOULOS, M. C. FERRO, D. U. TULYAGANOV, J. M. F. FERREIRA*
Department of Ceramics and Glass Engineering, University of Aveiro, 3810-193 Aveiro, Portugal
E-mail: jmf@cv.ua.pt

In the process of low-temperature sintering of AlN ceramics, the reaction of the sintering aids YF_3 and CaF_2 with superficial Al_2O_3, inherently contained in AlN lattice, results in formation of liquid phase. Nevertheless, the uniformly dispersed liquid phase is prone to migrate from the bulk to the surface of the samples, opposing densification. The analysis of the experimental results indicates that fresh liquid phase can continuously arrive from the bulk to the surface due to chemical reactions and crystallization which occur at the surface as well as wettalibilty and capillarity phenomena. The surface is depleted of liquid phase since the latter is consumed due crystallization and carbothermal reduction reactions with the elements of the atmosphere of the furnace N_2 and C, resulting in formation of a dense layer of crystals of $Al_2Y_4O_9$, $CaYAl_3O_7$ and Y_2O_3, grown perpendicularly to the surface. The chemical and structural features of this newly formed crystalline surface layer generate a significant difference of the wetting regimes and the capillary forces between the surface and the bulk, favouring pumping of the liquid from the bulk to the surface.

1. Introduction

The properties of aluminium nitride, such as high thermal conductivity, low dielectric constant, high electrical resistance and good matching of thermal expansion coefficient with silicon, indicate AlN as potential material for producing substrates and packaging materials in high power integrated circuits [1–3]. Nevertheless, AlN ceramics generally feature two weak points:

(a) The production of highly compacted pieces of highly pure AlN by pressureless sintering is generally very difficult.
(b) The low mobility of the oxygen atoms dissolved in the lattice of AlN lowers thermal conductivity. This is however an intrinsic feature of AlN since exposure of AlN-powder in air results in spontaneous formation of superficial Al_2O_3. Thus, AlN inherently contains Al_2O_3 [1, 4].

The fabrication of dense AlN ceramics utilizes sintering aids, mainly oxides but in several cases also non-oxides. Rare-earth and alkaline earth oxides have attracted the most of the interest [5, 6]. Sintering aids based on Ca and Y have been extensively investigated, but other oxides are also effective [5–9]. The liquid phase formed due to the sintering aids during sintering can have a dual effect: It provides better densification and improves thermal conductivity of sintered ceramics since it can react with dissolved oxygen and purify the lattice of AlN.

Nevertheless, it has been reported that the liquid phase formed in AlN ceramics is prone to migrate towards the surface [10, 11]. This work aims to shed light to this important phenomenon, which actually opposes the aim of sintering aids during low-temperature sintering processing of AlN ceramics. To the knowledge of the authors, there is still poor documentation of this phenomenon in the literature.

2. Materials and experimental procedure

In this work, the AlN powder used was prepared by combustion synthesis (Fujian Huaqing New Materials

*Author to whom all correspondence should be addressed.

Co. Ltd., China; purity $\geq$ 99wt%; average diameter 2.13 μm; analysis of the major trace elements in wt%: Fe 0.0126, Si 0.118, O 0.85). A mixture of powders, comprising (in wt%) 95% AlN, 2% CaF_2 (Beijing Chemical Co., 99%, Beijing, China) and 3% YF_3 (Zhujiang Smeltery, 99%, Guangzhou, China), was ball-milled in a planetary mill for 6 h using ethanol as mixing medium. After drying, binder (PVB) was added. The mixture was homogenized by dry milling in a mortar. Pellets with 50 mm diameter and 5 mm thickness were prepared by uniaxial die pressing. De-waxing was carried out at 600°C. The pellets were placed into BN crucible and then sintered at 1700°C for 3 h (heating rate $\sim$10 K/min and rapid cooling after sintering) in a furnace with graphite-heating element under flowing N_2 atmosphere.

The analyses were done at the surface, at cross sections (revealed by careful fracture of samples), in the bulk, and at subsurface areas of the samples. The term subsurface denotes the area located underneath the outermost original surface of the samples, which was revealed by simple grinding (the thickness of the superficial layer removed after grinding was roughly estimated to be $\sim$0.3 mm). Scanning electron microscopy was employed for microstructure observations (SEM, Philips-Fei, XL30-TMP, the Netherlands). The crystalline phases were identified by X-ray diffraction analysis (XRD, Bruker D8 Advance, Cu K_α, Germany). X-ray fluorescence was employed for elemental analysis (XRF, Bruker S4 Explorer, Germany). XRD and XRF analyses were carried out in low incidence angle mode. The bulk of the samples was analyzed by transmission electron microscopy (TEM, Hitachi H-9000 NA, Japan, equipped with energy dispersive analysis and electron diffraction analysis apparatus, EDS). To remove the superficial sintering skin, the samples were grinded and polished at both sides (final thickness of the sample $<$50 μm). Disks of appropriate diameter were cut and glued on Cu-ring supporters using an epoxy resin. The samples were ion-beam thinned in an ion milling apparatus (BAL-TEC, RES100, Switzerland).

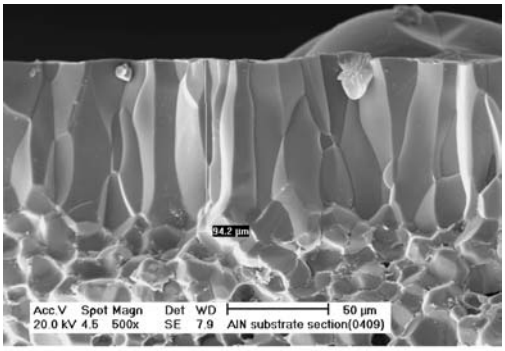

(a)

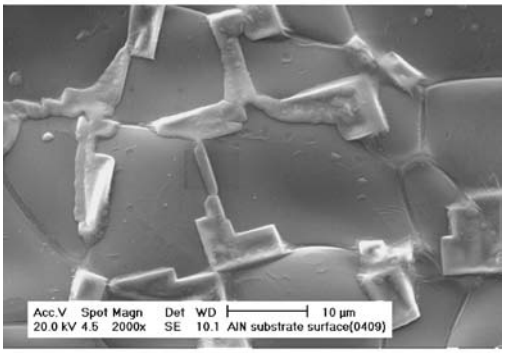

(b)

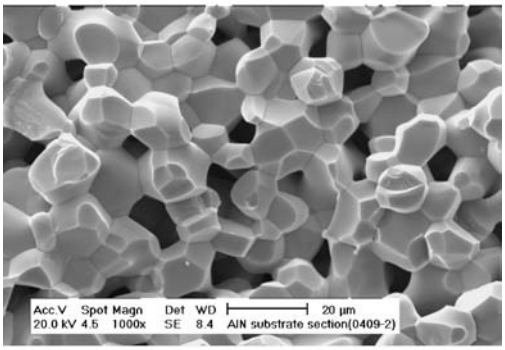

(c)

Figure 1 Microstructure observed (a) at cross section of fracture surface, (b) over top view and (c) in the bulk of sintered AlN pellets.

3. Results

After sintering, observation revealed that the samples were slightly warped. Moreover, their surface had a dark-bluish colour.

Fig. 1 presents typical microstructures observed at cross-sections revealed at fractured surfaces (a), top view (b) and in the bulk (c). The highly condensed and crystallized surface layer comprised elongated crystals ($\sim$100 μm) developed perpendicularly to the surface (Fig. 1a). The liquid phase, whose shape may evidence crystallization, was emerged at the surface at the grain boundaries (Fig. 1b). The crystals at the subsurface area (middle-bottom area in Fig. 1a) and the bulk (Fig. 1c), attributed to AlN, are similar but certainly different from the elongated crystals formed at the surface of the samples. Careful observation shows that liquid phase has completely infiltrated along the grain boundaries in the subsurface area (Fig. 1a) while the microstructure of the bulk features poor densification (Fig. 1c). In the latter case, careful observation can identify isolated islets of liquid phase of submicron dimensions at triple points of grain boundaries.

The X-ray spectra indicate that the investigated materials were well crystallized, since there was no evidence of glassy phase (Fig. 2). Neglecting the dominant peaks of AlN, high magnification of the intensity axis reveals that yttria (Y_2O_3) was formed at the surface of the pellets (Fig. 2a). The crystalline state of subsurface was different (Fig. 2b). With respect to the secondary phases, comparison of the intensities indicates a poorer crystalline regime of the subsurface than the surface. Subsurface contained no Y_2O_3 but mainly $Al_2Y_4O_9$, while traces of $CaYAl_3O_7$ might be also suggested.

The elemental analysis (Fig. 3) showed that the surface is considerably richer in Y and also in O than the subsurface. The lower concentration of Al and N in the surface than the subsurface indicates that the surface was enriched with elements involved in the liquid phase. The trace elements, probably dissolved in the

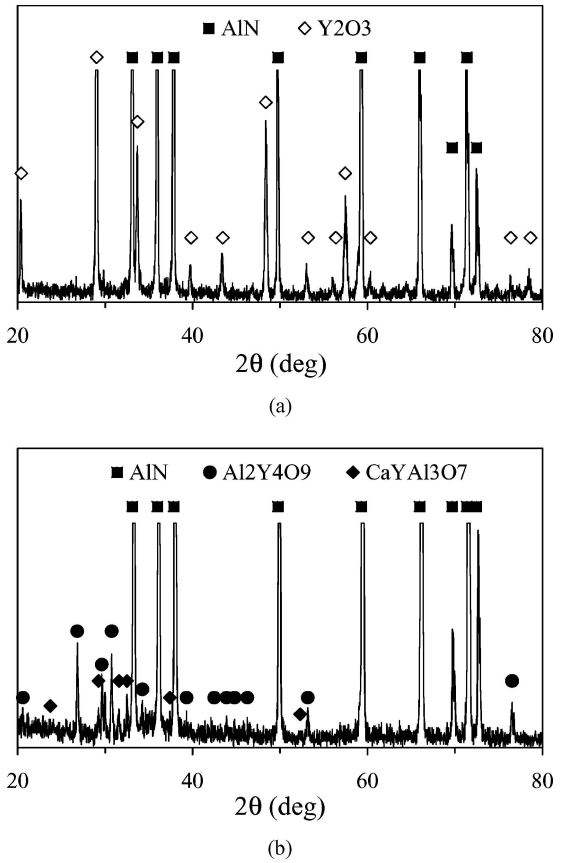

Figure 2 XRD analysis of (a) the surface and (b) the subsurface of the pellets. (Full scale (in cps) of the intensity axis: (a) 230; (b) 180; JCPDS cards: AlN 25-1133; Y_2O_3: 41-1105; $Al_2Y_4O_9$: 34-0368; $CaYAl_3O_7$: 49-0605).

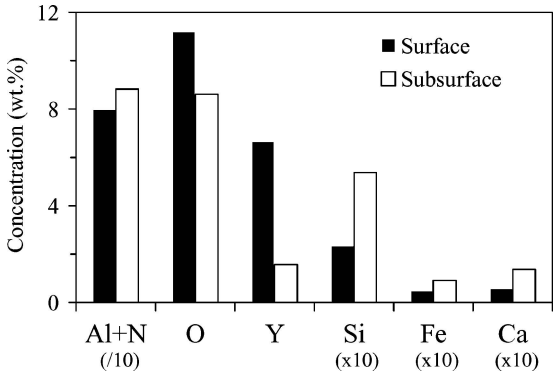

Figure 3 Elemental analysis (XRF) of the surface and the subsurface of AlN pellets. The first columns correspond to the sum of Al and N since the XRF analysis can hardly distinguish these two elements.

crystallized liquid phase, were preferably concentrated in the subsurface rather than at the surface. The formation of $CaYAl_3O_7$ only in the subsurface (Fig. 2b) seemingly agrees fairly well with the higher concentration of Ca in the subsurface (Fig. 3).

Fig. 4 presents the results of TEM analysis made in the bulk of the sintered samples. The darker areas indicate domains which feature higher atomic mass. Therefore, it is clear that the liquid phase produced during sintering and remained in the bulk after the end of the whole process was preferentially accumulated at the triple points of the AlN grains forming isolated islets. The grain boundaries have been entirely depleted

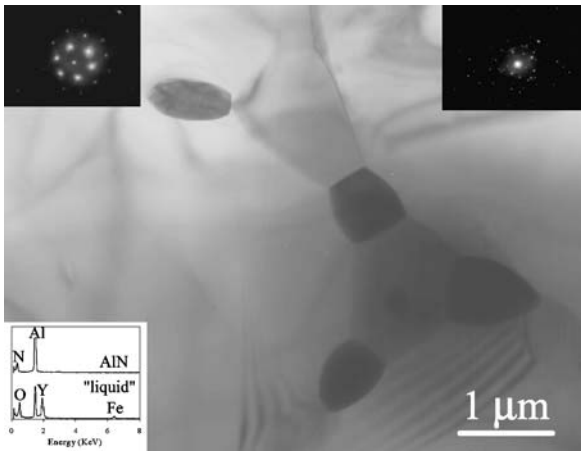

Figure 4 TEM image and EDS analyses of the bulk of sintered AlN pellets. The upper left hand inset corresponds to AlN grains (identified by the light colour areas in the main image) and the right hand inset to the crystallized glassy phase (dark colour areas).

of liquid phase. This result is a clear evidence of poor wetting between the liquid phase and the AlN grains. The right hand inset (EDS at the dark domains) confirms that the liquid phase was highly crystallized. EDS analysis (bottom left-hand inset) showed no element diffusion in the grains of AlN. The elemental analysis (by EDS) of the crystallized liquid phase was 47.0% O, 30.0% Al, 18.6% Y and 4.3% Fe (in at%), indicating a considerable enrichment of liquid phase in Fe.

4. Discussion

The presence of the sintering aids caused formation of liquid phase during sintering, which was crystallised afterwards. The phase diagrams between $Al_2O_3$and rare-earth oxides or alkaline-earth oxides (e.g. CaO) anticipate several phases over a wide range of temperature [12, 13]. In Y_2O_3 and YF_3 containing systems, the formation of liquid phases of yttrium aluminates, such as $AlYO_3$, $Al_5Y_3O_{12}$ and $Al_2Y_4O_9$, has been attributed to reactions with Al_2O_3 at elevated temperatures [10, 11, 14]. Accordingly, transient liquid-phase mechanism actually governed the rapid densification of AlN, whereby the superficial Al_2O_3 reacted with the sintering additives forming the liquid phase that was finally crystallized. This reaction certainly aids the purification of AlN from oxygen (i.e. from Al_2O_3) and favours the increase of thermal conductivity of the sintered ceramics. Virkar *et al.* [14] postulated that the use of sintering aids which have the highest chemical potential with respect to the reaction with Al_2O_3 to aluminates results in AlN ceramics with the highest thermal conductivity.

The experimental results showed that the liquid phase was extensively crystallized [15]. The exclusive presence of Y_2O_3 at the surface (Fig. 2a) may indicate the occurrence of carbothermal reduction reactions between the liquid phase and the C-rich N_2-atmosphere of the furnace:

$$2Al_5Y_3O_{12} + 5N_2 + 15C \rightarrow 3Y_2O_3 + 10AlN + 15CO \quad (1)$$

$$Al_2Y_4O_9 + N_2 + 3C \rightarrow 2Y_2O_3 + 2AlN + 3CO \quad (2)$$

In other words, it is proposed that the true phases directly precipitated from the reservoir of the liquid phase should be largely $Al_2Y_4O_9$ and traces of $CaYAl_3O_7$, which are well preserved (with regards to the influence of the atmosphere of the furnace) at the subsurface. If $Al_5Y_3O_{12}$ had been also formed, then it should have exclusively concentrated at the surface and then completely reacted with the elements of the furnace atmosphere to Y_2O_3, according to Equation 1. Earlier studies have shown that in the case of use of Y_2O_3 as sintering aid, $Al_5Y_3O_{12}$ is the primarily formed aluminate. In the case of high amount of Y_2O_3, the secondary phases are transformed following the order $Al_5Y_3O_{12}$, $AlYO_3$, $Al_2Y_4O_9$ and Y_2O_3 [11]. In the AlN-Y_2O_3-CaO ternary system, the phases, often encountered in the sintered pellets, are $Al_2Y_4O_9$, $CaYAl_3O_7$ and $CaYAlO_4$ [7–9].

Beyond purification, the experimental results indicate however that the liquid phase is prone to migrate from the bulk to the surface, causing pronounced chemical and structural inhomogeneity in the resulting material, with regards to the differences between the surface and the bulk. Nevertheless, the liquid phase should have been uniformly formed throughout the entire volume of the samples immediately after the reaction of the sintering aids with the dissolved Al_2O_3. Evaporation of liquid phase via carbothermal reduction in a C-containing N_2-atmosphere has been suggested as a cause of this inhomogeneity [16, 17]. The dense structure of the surface (Fig. 1a and b) indicates however low probability of this mechanism, since the bulk is apparently unlike to bare more intensive evaporation than the surface. Hence, this work proposes that the driving force for the migration of the liquid phase should deal with chemical potentials, crystallization, wettability and capillary forces.

With regards to the former two factors, the consumption of the first liquid phase, formed at the surface in the beginning of the process, due to the reaction with the elements of the atmosphere of the furnace (Equations 1 and 2) and crystallization, should have stimulated the migration of fresh liquid from the bulk to the surface. The formation of the thick and condensed crystalline surface layer and the orientation of the elongated crystals (Fig. 1a), the emerging liquid at the surface (Fig. 1b), the depletion of bulk of liquid phase (Fig. 1c), and the XRD spectra (Fig. 2) support this concept.

The formation of the first crystals at the surface immediately generates a great difference between the wetting regimes at the surface and the bulk because of the followings: The SEM images (Fig. 1) indicate that the pores at the surface crystallized layer are considerably narrower than the pores in the bulk. Therefore, much stronger capillary forces are expected to be developed at the surface layer than in the bulk. On the other hand, the TEM analysis (Fig. 4) indicated that the liquid phase poorly wets AlN. In the surface layer however, the walls of the capillary pores are made from a material directly derived from the liquid phase itself. Therefore, better wetting regime should be anticipated than that in the bulk. Consequently, the liquid phase should be prone to be pumped out from the bulk to the surface migrating from the region which features poorer wetting conditions and larger pores (i.e., weaker capillary forces) to the region which features better wettability and narrower pores (i.e., stronger capillary forces).

The fresh liquid phase which arrives at the surface crystallizes and reacts with the elements of the furnace atmosphere resulting in thickening of the superficial crystalline layer and further depleting of the bulk of liquid phase.

The difference of capillary forces between the surface and the bulk in conjunction with the agglomerated nature and the consequent poor sintering ability of the starting AlN powder most likely caused the observed warping effect, since capillary forces govern structural rearrangements during liquid phase sintering. Consequently, the shrinkage should be higher at the surface than in the bulk, where large (inter-agglomerates) pores (Fig. 1c) should oppose densification.

In this study, the TEM observations did no allow us to measure the exact wetting angle between AlN and the liquid phase. The direct measurement of contact angles in such type of systems is currently underway. Poor wettability of AlN has been reported in TEM studies with lanthanide aluminates, where the wetting angle between the liquid phase and AlN was 72.5° (after solidification) [11].

With regards to the kinetics of migration, suitable viscosity and fluidity of the liquid phase at the investigated temperature evidently facilitated the migration. Earlier studies have shown that the amount of liquid phase which migrates towards the surface increases over increasing sintering temperature and holding time [10, 11]. Therefore, in prolonged experiments, the liquid phase has enough time to empty the bulk and migrate to the surface.

In earlier studies it has been reported that in the case of high Y_2O_3 concentration, the isolated AlN grains are usually spherical in shape, while at low concentration of aluminate-phases, the AlN grains usually form equiaxed polyhedra [11]. The aluminate liquid phase is preferably gathered at the corners of AlN grains and spread along the edges of the grains as the volume fraction increases, assisting densification of the green body. Grain growth is directed towards the surface because the shrinkage of the pellets takes place rapidly in the beginning of sintering [10].

5. Conclusions

Transient liquid-phase mechanism, which occurs via formation of liquid phase due to reaction of the superficial Al_2O_3 with the sintering additives YF_3 and CaF_2, takes place during pressureless sintering of AlN ceramics and apparently favours the purification of AlN ceramics from Al_2O_3. With regard to densification however, the experimental results indicate that the liquid phase migrates from the bulk to the surface. Chemical reactions, crystallization, wettalibilty and capillarity should govern the migration. Crystallization and carbothermal reduction reactions of the liquid phase

with the elements of the atmosphere of the furnace N_2 and C result in formation of a dense layer of crystals of $Al_2Y_4O_9$, $CaYAl_3O_7$ and Y_2O_3, grown perpendicularly to the surface. Both chemical reactions and crystallization have a dual effect in liquid phase migration: (a) They result in depletion of liquid phase at the surface, stimulating therefore migration of fresh liquid phase from the bulk to the surface. (b) They create a significant difference of the wettability and the capillary forces between the surface and the bulk. Therefore, liquid phase is prone to empty the bulk and be pumped out to the surface.

References

1. G. A. SLACK, *J. Phys. Chem. Solids.* **34** (1973) 321.
2. L. M. SHEPPARD, *Am. Ceram. Bull.* **69** (1990) 1801.
3. Y. BAIK and R. A. L. DREW, *Key Eng. Mater.* **122–124** (1996) 553.
4. G. A. SLACK, R. A. TANZILLI, R. O. POHL and J. W. VANSDERANDE, *J. Phys. Chem. Solids* **48** (1987) 641.
5. K. KOMEYA, H. INOUE and A. TSUGE, *J. Am. Ceram. Soc.* **54** (1974) 411.
6. K. KOMEYA, A. TSUGE, H. INOUE and H. ONTA, *J. Mater. Sci. Lett.* **1** (1982) 325.
7. L. QIAO, H. ZHOU, H. XUE and S. WANG, *J. Eur. Ceram. Soc.* **23** (2003) 61.
8. Y. LIU, H. ZHOU, L. QIAO and Y. WU, *J. Mater. Sci. Lett.* **18** (1999) 703.
9. Y. C. LIU, H. P. ZHOU and L. QIAO, *J. Inorg. Mater.* **15** (2000) 619 (in Chinese).
10. L. QIAO, H. P. ZHOU, Y. C. LIU and Y. D. WANG, *Mater. Eng.* **10** (2000) 7 (in Chinese).
11. T. B. JACKSON, A. V. VIRKAR, K. L. MORE, R. B. DINWIDEIE and R. A. CUTLER, *J. Am. Ceram. Soc.* **80** (1997) 1421.
12. Figures 9115–9800, in "Phase Equilibria Diagrams, Phase Diagrams for Ceramics", Vol. XI Oxides, edited by R. S. Roth (The American Ceramic Society,1995) p. 356.
13. Figures 9801-10244, "in Phase Equilibria Diagrams, Phase Diagrams for Ceramics", Vol. XII Oxides, edited by A. E. McHale and R. S. Roth (The American Ceramic Society, 1996), p. 199.
14. A. V. VIRKAR, T. B. JACKSON and R. A. CUTLER, *J. Am. Ceram. Soc.* **72** (1989) 2031.
15. R. FU, H. ZHOU and L. CHEN, *Mater. Sci. Eng.* **A266** (1999) 44.
16. K. WATARI, M. KAWAMOTO and K. ISHIZAKI, *J. Mater. Sci.* **26** (1991) 4727.
17. P. GREIL, M. KULIG and D. HOTZA, *J. Eur. Ceram. Soc.* **13** (1994) 229.

Received 31 March
and accepted 18 July 2004